# Ion diffusion coefficient measurements in nanochannels at various concentrations

Junrong Wang, Li Zhang, Jianming Xue, and Guoqing Hu

Citation: Biomicrofluidics **8**, 024118 (2014); doi: 10.1063/1.4874215
View online: http://dx.doi.org/10.1063/1.4874215
View Table of Contents: http://scitation.aip.org/content/aip/journal/bmf/8/2?ver=pdfcov
Published by the AIP Publishing

# Ion diffusion coefficient measurements in nanochannels at various concentrations

Junrong Wang,[1] Li Zhang,[2] Jianming Xue,[3,a)] and Guoqing Hu[1,a)]
[1]*State Key Laboratory of Nonlinear Mechanics, Institute of Mechanics, Chinese Academy of Sciences, Beijing 100190, China*
[2]*Research and Development Center, Synfuels China Technology Co., Ltd., Beijing 101407, China*
[3]*State Key Laboratory of Nuclear Physics and Technology, Peking University, Beijing 100871, China*

(Received 25 January 2014; accepted 21 April 2014; published online 30 April 2014)

Diffusion is one of the most fundamental properties of ionic transport in solutions. Here, we present experimental studies and theoretical analysis on the ion diffusion in nanochannels. Based on Fick's second law, we develop a current monitoring method to measure ion diffusion coefficient of high solution concentrations in nanochannels. This method is further extended to the cases at medium and low concentrations. Through monitoring ionic current during diffusion, we obtain diffusion coefficients of potassium chloride solution at different concentrations in nanochannels. These diffusion coefficients within the confined space are close to theirs bulk values. It is also found that the apparent ion diffusion equilibrium in the present experiments is very slow at low concentration, which we attribute to the slow equilibrium of the nanochannel surface charge. Finally, we get a primary acknowledge of the equilibrium rate between the nanochannel surface charge and electrolyte solution. The results in this work have improved the understanding of nanoscale diffusion and nanochannel surface charge and may be useful in nanofluidic applications such as ion-selective transport, energy conversion, and nanopore biosensors. © *2014 AIP Publishing LLC*.
[http://dx.doi.org/10.1063/1.4874215]

## I. INTRODUCTION

Rapid advances in micro- and nanofabrication techniques have made it possible to produce various types of nanofluidic devices, such as nanochannels or nanopores, with at least one characteristic dimension below 100 nm.[1,2] One of the great challenges in nanofluidic applications is to exploit the unique transport properties within nanoscale confinement.[3–5] Ion diffusion in aqueous solutions forms the fundamental transport process in nature. There exist several experimental methods to determine the diffusion coefficient of ions in aqueous solutions, including optical methods,[6,7] dispersion methods,[8] chronoamperometric methods,[9] hydrodynamic methods,[10] etc. However, most of them are complex and not suitable to be used in nanochannel measurement.

In the recent years, experiment studies[11–13] have demonstrated that the apparent diffusion coefficients of fluorescently labeled proteins or nanoparticles in a nanochannel may be orders of magnitude lower than their bulk diffusion coefficients. Such disparity is understandable since in those studies the size of biomolecule or nanoparticle is comparable to the characteristic length scale of the nanofluidic systems and thus cannot be treated as point particles. Molecular dynamics simulations have also shown that the diffusion coefficients of ions decrease significantly inside typical biological nanopores that have narrow constrictions of diameter of 1–2 nm.[14,15]

[a)]Authors to whom correspondence should be addressed. Electronic addresses: jmxue@pku.edu.cn and guoqing.hu@imech.ac.cn.

 

The lower diffusion coefficients are probably due to the strong interactions of the water molecules and the ions with nanopore walls.[14,16]

However, in nanochannels with dozens of nanometer or larger scale, whether the diffusion will be affected by the confinement is still unclear. There are three types of intermolecular forces in liquids near a solid surface: steric interactions (in range of ~0.1–2 nm), van der Waals forces (in range of ~0.1–50 nm), and electrostatic forces (in range of Debye length, ~1–100 nm). Apart from steric interactions, the other two forces can be modeled by continuum approximation.[17] Daiguji[18] suggested that continuum dynamics is an adequate description of ionic transport phenomena for dimension scale larger than ~5 nm. In the continuum modeling, some works[19–23] assumed ion diffusion coefficients to be the same as their bulk values, while other works[24–26] chose different apparent diffusion coefficients to fit their experimental data. Using a continuum model with bulk diffusion coefficients of ions, Qian and co-workers investigated the diffusiophoretic motion of a nanoparticle caused by applying a salt concentration gradient in a nanopore with diameters ranging from 8 nm to 20 nm.[19–21] Siwy *et al.*[24] did experimental research on asymmetric diffusion through synthetic conical polyethylene terephthalate (PET) nanopore with minimum radii of 1.5 nm. In order to fit the calculated diffusion currents to the experimental data, they adjusted the ion diffusion coefficients and estimated a quarter of bulk value for anionic diffusion coefficient in the nanopore. Hirono *et al.*[25] estimated that the ion diffusion coefficients might be about half of its bulk values in rock nanoscale pores with diameters below 100 nm. Yossifon and Chang,[26] on the other side, adopted a high ion diffusion coefficient of ~2 times of its bulk value when they researched ion-depletion phase in a 200 nm deep nanochannel. However, there is no accurate experiment yet to evaluate those assumptions by measuring the ionic diffusion directly.

Several experiments were carried out to get apparent diffusion coefficients based on Fick's law in nanochannels.[27–30] The experiments were designed as the ionic flux goes from one end of the nanochannels with high salt concentration to the other end with low salt concentration. The apparent diffusion coefficients were usually orders of magnitude lower than its bulk values. For example, Bluhm and co-workers[27,28] have shown that the apparent diffusion coefficients of cations diffusion through an alumina membrane containing 20 nm diameter nanochannels might be one order of magnitude lower than their bulk values. Since nanochannels have a high surface-to-volume ratio, they attributed the low apparent diffusion coefficients to positive surface charge of the alumina nanochannels in which cationic concentration was significantly smaller than the bulk concentration. Although the apparent diffusion coefficient to some extent represents the diffusion behavior such as diffusion flux in nanochannels, it cannot be considered as the real diffusion coefficient.

Surface charge plays an important role on ionic transport in nanochannels, especially at low salt concentrations.[31] Silica is one of the most popular materials used in fabricating nanochannels. The surface charge density of silica nanochannels is usually simply considered to be a constant value at different bulk salt concentrations.[31–33] However, previous theoretical studies have demonstrated that the charge densities on the silica surface are results of chemical equilibrium between the surface and the solution, known as "charge regulation,"[34–36] which indicates that the silica surface charge density is related to bulk salt concentration.

Experimental and theoretical studies have focused on the surface charge density of silica nanochannels at different bulk concentrations.[37–40] However, the rate of the equilibrium between the wall charge and solution is seldom investigated. Zangle *et al.*[41] thought that the equilibrium between the nanochannel surface charge and bulk solution was not achieved instantaneously in their experiments. Raider *et al.*[42] found that the kinetics of ionic adsorption on silicon dioxide surface was a slow process, and this process could take several hours for a neutral solution. Duan and Majumdar[43] observed that it took about 10 h for the conductance of their nanochannels to reach a steady state. Therefore, the slow equilibrium of surface charge may significantly affect ion transport phenomena like ion diffusion in nanochannels.

In this paper, we have experimentally and theoretically studied the constrained diffusion of ions in nanochannels. By monitoring the ionic current, we present a simple technique to measure the diffusion coefficient of potassium chloride (KCl) solution at high concentrations in

nanochannels. The method is then extended to the cases at medium and low bulk concentrations by theoretically analyzing ionic governing equations and ionic current in nanochannels. Our theory points out that the change of surface charge affect ion diffusion at relatively low concentrations, which is observed in our experimental measurements. Finally, we get the equilibrium rate between the nanochannel surface charge and solution at low salt concentrations.

## II. THEORY

### A. Current monitoring method

Diffusion is a passive motion of molecules or ions from regions of higher concentration to regions of lower concentration. Ion diffusion in a nanochannel and its electrical measurement used in the present study are schematically illustrated in Fig. 1. Initially, the reservoirs and the nanochannel are filled with a certain concentration of KCl solution. If the solution in both reservoirs is replaced to another concentration, the ions will diffuse in the nanochannel to achieve new equilibrium.

We first consider high bulk concentrations cases, in which the electric double layer (EDL) and surface charge on the nanochannel walls can be neglected.[3,31] Thus, the diffusion process can be simply described by Fick's second law,

$$\frac{\partial C(x,t)}{\partial t} = \frac{\partial}{\partial x} D \frac{\partial C(x,t)}{\partial x}, \tag{1}$$

with the initial condition

$$C(x,0) = C_0, \tag{2}$$

where $C$ is the concentration of the electrolyte solution and $D$ is the ion diffusion coefficient.

Since the volume ratio of the reservoirs to the nanochannel is very huge, we can take the solution concentration in reservoirs as invariable during diffusion process. Thus, at both the ends of the nanochannel, the concentration boundary conditions are set as

$$C(0,t) = C_1, \quad C(L,t) = C_1, \tag{3}$$

where $L$ is the length of the nanochannel.

According to Harned and Nuttall,[44] the ion diffusion coefficient of infinite dilution KCl solution at 293.16 K is $D = 1.77 \times 10^{-9}$ m$^2$/s. It slightly decreases with increased concentration and can be calculated as $D = 1.63 \times 10^{-9}$ m$^2$/s for 100 mM KCl or $D = 1.62 \times 10^{-9}$ m$^2$/s for 200 mM KCl. In this work, we assume constant ion diffusion coefficient during each diffusion experiment. Then Eq. (1) becomes

$$\frac{\partial C(x,t)}{\partial t} = D \frac{\partial^2 C(x,t)}{\partial x^2}. \tag{4}$$

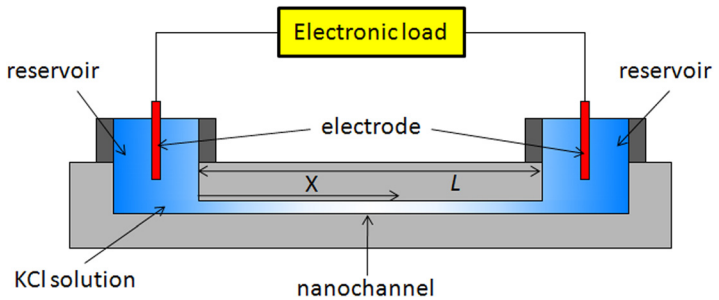


FIG. 1. Schematic diagram of ion diffusion in a nanochannel and electrical measurement system.

From Eqs. (2)–(4), the concentration of the electrolyte solution in the nanochannel can be solved and given by the following series form:

$$\frac{C(x,t)-C_1}{C_0-C_1}=\sum_{n=1}^{\infty}\frac{2}{n\pi}\left[1+(-1)^{n+1}\right]\sin\frac{n\pi x}{L}\exp\left(-\frac{Dn^2\pi^2}{L^2}t\right)$$
$$=\frac{4}{\pi}\left[\sin\frac{\pi x}{L}\exp\left(-\frac{D\pi^2}{L^2}t\right)+\frac{1}{3}\sin\frac{3\pi x}{L}\exp\left(-9\frac{D\pi^2}{L^2}t\right)+\cdots\right]. \quad (5)$$

Integrating Eq. (5) along the nanochannel length yields

$$\frac{\overline{C(t)}-C_1}{C_0-C_1}=\frac{8}{\pi^2}\left[\exp\left(-\frac{D\pi^2}{L^2}t\right)+\frac{1}{9}\exp\left(-9\frac{D\pi^2}{L^2}t\right)+\cdots\right], \quad (6)$$

where $\overline{C(t)}=\frac{1}{L}\int_0^L C(x,t)dx$ denotes the average concentration along the nanochannel length.

At high bulk concentrations, the surface conductance is negligible so that the nanochannel conductance is solely the bulk conductance,[31,32] which is linear with the average ionic concentration. Therefore, we can measure the nanochannel conductance with a transient low voltage to get average ionic concentration in the nanochannel. The externally applied voltage across the nanochannel shall be very low and the duration is very short and thus it does not cause extra ion migration. Under a constant externally applied voltage, the electrical current depends linearly on the average concentration. From Eq. (6), the current versus diffusion time can be obtained as

$$\frac{I(t)-I_1}{I_0-I_1}=\frac{8}{\pi^2}\left[\exp\left(-\frac{D\pi^2}{L^2}t\right)+\frac{1}{9}\exp\left(-9\frac{D\pi^2}{L^2}t\right)+\cdots\right], \quad (7)$$

where $I_0$ denotes the initial current and $I_1$ denotes the current when the ion diffusion is completed. If the value of $D\pi^2t/L^2$ reaches 0.5, the ratio of the second term to the first term on the right-hand side of Eq. (7) is about 0.2%. Therefore, at $D\pi^2t/L^2>0.5$ (for example, with $D=1.6\times10^{-9}$ m$^2$/s and $L=6$ mm, $t>1140$ s), we can only keep the first term on the right-hand side of Eq. (7), and get a simple form

$$I(t)=I_1-\frac{8(I_1-I_0)}{\pi^2}\exp\left(-\frac{D\pi^2}{L^2}t\right). \quad (8)$$

The characteristic time $\tau$ can be calculated by fitting the experimental data with the mono-exponential curve $I=I_1-A\exp(-t/\tau)$. Subsequently, we can obtain the ion diffusion coefficient as $D=L^2/(\tau\times\pi^2)$. We call this method the current monitoring method.

The underlying principle of this current monitoring method is similar to the technique used in microchannels to determine the zeta potential.[45] Tang *et al.* analyzed electro-osmotic flow displacement between two solutions in a uniformly charged microchannel and examined how solution conductivity difference plays roles in the current monitoring method.[46] Harned and Nuttall[47] used a conductance method based on a similar principle to measure the diffusion coefficients of electrolytes in a macro channel device. It was difficult for them to eliminate convection impact upon introducing the electrolytic solution and turbulent flow derived from non-uniform temperature. However, those difficulties can be overcome in our experiment due to the unique properties of nanochannel such as high flow resistance and extremely low Reynolds number.

Since our current monitoring method is derived at high bulk concentrations, it has to be modified to deal with the cases at medium and low bulk concentrations. We will discuss it later in detail.

### B. Governing equations

Since the thickness of EDL cannot be neglected at medium and low bulk concentrations in a nanochannel, ionic concentration gradient exists across the channel height induced by the

EDL. As a result, we cannot directly use Fick's second law to describe the diffusion process. Based on the continuum approximation, the ionic transport in a nanochannel can be described using the Poisson-Nernst-Planck (PNP) equations and the Navier–Stokes (NS) equations,[19,20,23,48]

$$\nabla^2\phi = -\frac{\rho_e}{\varepsilon_0\varepsilon_r}, \tag{9}$$

$$\frac{\partial c_i}{\partial t} + \nabla\cdot\mathbf{J}_i = \frac{\partial c_i}{\partial t} + \nabla\cdot\left(-D_i\nabla c_i + \mathbf{u}c_i - \frac{z_iFD_i}{RT}c_i\nabla\phi\right) = 0, \tag{10}$$

$$\nabla\cdot\mathbf{u} = 0, \tag{11}$$

$$\rho\left(\frac{\partial\mathbf{u}}{\partial t} + \mathbf{u}\cdot\nabla\mathbf{u}\right) = \mu\nabla^2\mathbf{u} - \nabla p - \rho_e\nabla\phi, \tag{12}$$

where $\phi$ is the electrical potential, $\varepsilon_0$ is the electrical permittivity of vacuum, $\varepsilon_r$ is the relative permittivity of solution, $F$ is the Faraday constant, $R$ is the molar gas constant, and $T$ is the temperature; $c_i$, $\mathbf{J}_i$, $D_i$, and $z_i$ are the concentration, flux, diffusivity, and valence of the each ionic species, respectively; $z_iFD_i/RT$ is the electrophoretic mobility obtained from the Nernst–Einstein relation; $\mathbf{u}$, $\mu$, $\rho$, and $p$ are the velocity vector, dynamic viscosity, density, and pressure, respectively. Here, $\rho_e$ is charge density of the ionic species and is given by $\rho_e = F\sum_{i=1}^{n} z_ic_i$, where $n$ is the number of ionic species involved in the system.

Since the effect of the external transient electric field on diffusion can be neglected, the fluid velocity is assumed to be zero during diffusion. Considering a two-dimensional problem, Eq. (10) is rewritten as

$$\frac{\partial c_i}{\partial t} = D_i\frac{\partial^2 c_i}{\partial x^2} + \frac{z_iFD_i}{RT}\frac{\partial}{\partial x}\left(c_i\frac{\partial\phi}{\partial x}\right) + D_i\frac{\partial^2 c_i}{\partial y^2} + \frac{z_iFD_i}{RT}\frac{\partial}{\partial y}\left(c_i\frac{\partial\phi}{\partial y}\right), \tag{13}$$

where $x$ denotes the direction along the channel axis and $y$ denotes the transverse coordinate originating from the channel axis. The potential gradient in the $x$-direction is induced by diffusion when cations and anions in the electrolyte have different diffusion fluxes through the channel.[49,50] If the cations diffuse more rapidly than anions, the concentrated solution will be negatively charged and the dilute solution will be positively charged, resulting in a double layer of negative and positive charges between the two solutions. Therefore, a potential difference called diffusion potential will develop.

At high bulk concentrations, the thickness of EDL is negligible compared to the channel height, resulting in $\partial\phi/\partial y = 0$, $D_i\partial^2 c_i/\partial y^2 = 0$, and $c_{K^+} = c_{Cl^-} = c_{bulk}$ in the nanochannel. Therefore, Eq. (13) is reduced to

$$\frac{\partial c_{K^+}}{\partial t} = D_{K^+}\frac{\partial^2 c_{K^+}}{\partial x^2} + \frac{FD_{K^+}}{RT}\frac{\partial}{\partial x}\left(c_{K^+}\frac{\partial\phi}{\partial x}\right), \tag{14}$$

$$\frac{\partial c_{Cl^-}}{\partial t} = D_{Cl^-}\frac{\partial^2 c_{Cl^-}}{\partial x^2} - \frac{FD_{Cl^-}}{RT}\frac{\partial}{\partial x}\left(c_{Cl^-}\frac{\partial\phi}{\partial x}\right). \tag{15}$$

Multiplying Eq. (14) by $D_{Cl^-}$ and multiplying Eq. (15) by $D_{K^+}$ and then adding the two equations together, we can get

$$\frac{\partial c_{bulk}}{\partial t} = D\frac{\partial^2 c_{bulk}}{\partial x^2}, \tag{16}$$

where $D = 2D_{K^+}D_{Cl^-}/(D_{K^+} + D_{Cl^-})$ is the diffusion coefficient of KCl solution. Equation (16) is then the same as Fick's second law.

At medium and low bulk concentrations, there is intrinsic electric field and concentration gradient in the *y*-direction (across the channel height) stemming from surface charge. Taking no ions penetration through the nanochannel walls, we integrate Eq. (13) in the *y*-direction and eliminate the last two terms on the right-hand side,[51]

$$\frac{\partial \overline{c_i}}{\partial t} = D_i \frac{\partial^2 \overline{c_i}}{\partial x^2} + Q, \tag{17}$$

$$Q = \frac{1}{h}\int_{-h/2}^{h/2} \frac{z_i F D_i}{RT}\frac{\partial}{\partial x}\left(c_i \frac{\partial \phi}{\partial x}\right) dy, \tag{18}$$

where $\overline{c_i} = \frac{1}{h}\int_{-h/2}^{h/2} c_i dy$ indicates the average ionic concentration in the *y*-direction. The source term $Q$ is related to diffusion potential. Because of the overall electroneutrality requirement, the difference of the average ionic concentrations between $K^+$ and $Cl^-$ is determined by the surface charge density. It should be noted that the asymmetry in the diffusion coefficients of the cations and anions, leading initially to different ionic fluxes, will build up a potential gradient along the *x*-direction. However, since the diffusion coefficients of $K^+$ and $Cl^-$ are approximately equal, it is reasonable to assume that equal cations and anions enter into the nanochannel from the reservoirs, if the surface charge does not change much during the diffusion process. Therefore, the diffusion potential can be neglected and $Q$ term in Eq. (17) can be assumed zero, leading to

$$\frac{\partial \overline{c_{K^+}}}{\partial t} = D_{K^+} \frac{\partial^2 \overline{c_{K^+}}}{\partial x^2}, \tag{19}$$

$$\frac{\partial \overline{c_{Cl^-}}}{\partial t} = D_{Cl^-} \frac{\partial^2 \overline{c_{Cl^-}}}{\partial x^2}. \tag{20}$$

When equal $K^+$ ions and $Cl^-$ ions diffuse into the nanochannel, we can get $\partial \overline{c_{K^+}}/\partial t = \partial \overline{c_{Cl^-}}/\partial t$. Then Eqs. (19) and (20) can be merged into

$$\frac{\partial(\overline{c_{K^+}} + \overline{c_{Cl^-}})}{\partial t} = D \frac{\partial^2(\overline{c_{K^+}} + \overline{c_{Cl^-}})}{\partial x^2}, \tag{21}$$

where $D$ is already defined for Eq. (16).

If the surface charge changes significantly during a diffusion process, the diffusion potential cannot be neglected. In this case, the real diffusion coefficients cannot be measured with the present current monitoring method. However, we can get the changing rate of the surface charge when the change of surface charge dominates the diffusion process. Actually, a concentration gradient does exist along the nanochannel during the diffusion process, resulting in different local pH. However, the surface charge on the nanochannel walls does not instantaneously achieve equilibrium with the local pH, as pointed out in previous experimental studies.[42,43] Thus, we only consider the total change of surface charge of the whole nanochannel in the present work, rather than the local change. The nonuniform effect of the local pH on the nanochannel surface charge, such as the nonuniform or even discontinuous surface charge,[52] will be carefully considered in our future work.

### C. Electrical current analysis

At medium and low bulk concentrations, the nanochannel conductance is not linear with the bulk concentration due to the channel surface conductance. A commonly used approximate expression for the ionic current in a nanochannel is given by Schoch and co-workers.[32,33] Their expression is rewritten below:

$$\frac{I}{E_x} = F\left(\frac{FD_{K^+}}{RT} + \frac{FD_{Cl^-}}{RT}\right) c_{bulk} hw + 2\frac{FD_{K^+}}{RT}\sigma w, \tag{22}$$

where $E_x$ is the applied axial electric field, $\sigma$ is the surface charge density of the nanochannel; $h$ and $w$ is the height and width of the nanochannel, respectively. The first term on the right-hand side of Eq. (22) shows that the ionic current in a nanochannel at high concentrations is dominated by the nanochannel geometry and ionic concentration. The second term illustrates that, at low electrolyte concentrations, the ionic current is mainly governed by surface charge density of the nanochannel. However, this approximation only considers the electrophoretic current.

To get more accurate analysis, we integrate the ionic fluxes over the nanochannel cross-section to obtain the ionic current. According to Kirchhoff's first law, the ionic current is identical everywhere along the nanochannel. At the middle cross section of the nanochannel, the diffusion current is zero and thus the ionic current can be expressed as

$$\begin{aligned} I &= \int_{-h/2}^{h/2} F(J_{K^+} - J_{Cl^-})dy \\ &= \int_{-h/2}^{h/2} F(u_x c_{K^+} - u_x c_{Cl^-})dy + \int_{-h/2}^{h/2} F\left(\frac{FD_{K^+}}{RT} c_{K^+} E_x + \frac{FD_{Cl^-}}{RT} c_{Cl^-} E_x\right)dy. \end{aligned} \tag{23}$$

The first term on the right-hand side of Eq. (23) represents a contribution from the electro-osmotic flow, while the second term on the right-hand side stems from the ionic electrophoresis. The electrophoretic current is directly proportional to the ionic concentration, but the electro-osmotic current is not, which induces a non-linear relation between the average ionic concentration and the ionic current. If the electro-osmotic current can be considered as invariant during a diffusion process, we can also get the variation of the average ionic concentration in the nanochannel from the variation of the ionic current. Further, we use numerical simulation to investigate the influence of the electro-osmotic current in Results and discussion.

## III. EXPERIMENTAL

### A. Nanochannel fabrication

We fabricated nanofluidic devices in glass wafers (4″ PYREX 7740, 0.5 mm thick) using conventional MEMS processing techniques. The whole process started with a glass wafer. First, nanochannels were patterned on the wafer by standard photolithography. Briefly, a glass wafer was cleaned in acetone, ethanol, and a piranha solution ($H_2SO_4$:$H_2O_2$ = 7:3) for 10 min, respectively. Then it was rinsed in deionized water, spun dry with nitrogen gas, and primer-treated with hexamethyldisilazane (HMDS) as an adhesion layer. Then it was coated with a thin layer of photoresist (AZ5214). The photoresist was soft-baked at 95 °C for 90 s. The nanochannels were then transferred from a photomask to the photoresist film using a mask aligner (SUSS MA6/BA6, Germany). After UV exposure, the wafer was developed with developer solution (TMAH) for 40 s.

Before the etching step, an oxygen plasma machine was performed to remove photoresist residue left over after photoresist development to avoid uneven etching.[53] Next, we etched the wafer with an ion beam etching (IBE) machine through the opened photoresist area. The remaining photoresist was removed in acetone after etching. Thus, the etch depth is the height of nanochannels. The etch rate of the glass wafer was about 15 nm/min. And the selectivity of the IBE between the photoresist and the glass wafer was about 1:1. So, we could get a low etch rate to control etch depth easily and attain a small surface roughness.

Another glass wafer was drilled 2-mm-diameter holes with diamond driller as liquid access holes. Finally, the etched glass substrate and the glass cover were cleaned in piranha solution for 10 min. After rinsing in deionized water, the two glass wafers were then aligned and pressed together to make a spontaneous bonding. Thermal bonding was achieved by annealing in a furnace at 540 °C for about 6 h.[54]

We used a surface profilometer to measure the height of nanochannels before bonding. The height of nanochannels was about 65 ± 2 nm. The cross-sectional scanning electron microscopy

(SEM) images of nanochannels after bonding are shown in Fig. 2. It can be seen that there is no collapse or significant change of the depth after bonding.

Plastic ports used as reservoirs were attached with Silicone rubber to facilitate injection of fluids into nanochannels.

### B. Conductance measurement

In our experiments, the device had two large reservoirs connected by 40 nanochannels: each is $6 \pm 0.1$ mm long (between two reservoirs), $65 \pm 2$ nm high, and $5 \pm 0.5$ $\mu$m wide (totally $200 \pm 20$ $\mu$m wide).

The electrolytes used were KCl solutions prepared with deionized water. Different concentrations from 0.2M to 0.01 mM KCl were used. The pH values of the KCl solution were kept as 6.5. Ag/AgCl electrodes were used on both reservoirs to measure the ionic current as shown in Fig. 1. Before measurement, the reservoirs were filled with the chosen electrolyte solution. We carefully balanced the liquid levels at both ends to minimize the pressure-driven flow and used Parafilm M sealing film to enclose the reservoir to avoid evaporation. After waiting enough time to achieve ion equilibrium, the current was acquired by a patch clamp (Axon 200B, Molecular Devices, Inc.). The patch clamp operated in voltage-clamp mode with a 1 kHz low pass Bessel filter. The nanochannel conductance was obtained by linearly fitting the I-V curves, which were recorded by scanning the applied voltage from $-0.8$ V to $+0.8$ V with a step of 0.2 V. The temperature of the experiment environment was 20 °C.

The nanochannel conductances at different concentrations are displayed in Fig. 3. At high concentrations, the measured conductance increases linearly with concentration, following the bulk conductivity of the solutions. At low concentrations, however, the conductance only exhibits small variations with the concentration. It is worth noting that although the nanochannel conductance is generally considered to be dominated by the surface conductance only when the EDL overlap occurs, the surface conductance becomes significant at low concentrations even without EDL overlap.[31,33] The measured channel conductance agrees with the reported literatures.[37,38]

### C. Ion diffusion experiments

Initially, the reservoirs were filled with a certain concentration KCl solution. After waiting more than 10 h for the attainment of ion equilibrium, we replaced the solution of both reservoirs to another concentration. The ions diffuse in the nanochannels due to the concentration gradient. We monitored ionic current through the nanochannels at an applied transient low voltage during diffusion process.

The current was measured at the interval of 2 min. At each measurement, the voltage applied across the nanochannels was scanned from $-0.5$ V, 0 V, and $+0.5$ V, and each voltage step lasted for 2 s. We used the difference of current between 0 V and $+0.5$ V as the ionic current in our experiments below.

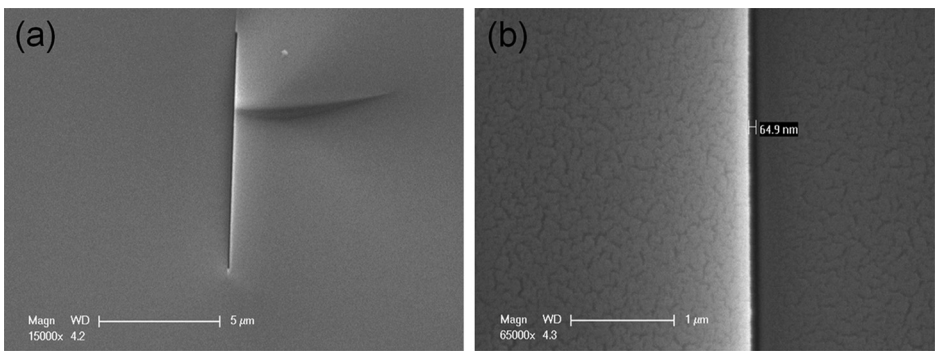


FIG. 2. (a) Cross-sectional SEM images of a nanochannel. (b) Magnified image of (a).

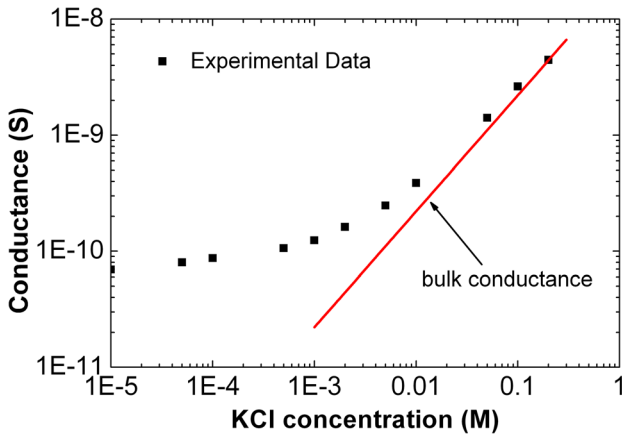


FIG. 3. Nanochannel conductance as a function of the electrolyte concentration.

Since the electrophoretic mobilities of $K^+$ and $Cl^-$ are about $6.3 \times 10^{-8}$ $m^2/(V \cdot s)$ at 293 K, under the applied voltage of 0.5 V for 2 s, the ions only move approximately 10 $\mu$m that is very small compared to the channel length of 6 mm. In addition, negative and positive voltages were alternatively applied to eliminate the impact of ionic electrophoresis and electro-osmotic flow. We also did experiments with lower applied voltage (i.e., 0.2 V) and got almost identical results. Therefore, we can safely neglect the impact of the transient applied voltage on diffusion in our experiments.

## IV. RESULTS AND DISCUSSION

### A. High concentrations

First, we tested the reliability of our experimental system. For ionic equilibrium at the 200 mM KCl, we monitored the ionic current with a 0.5 V applied voltage lasting for only 2 s at 2-min interval, as shown in Fig. 4. It can be seen that the maximal relative variation of the ionic current is about 1%. The ionic current experiences a relatively large reduction at the first few minutes. We believe that such change is a result of the slight variation of surface charge under the small electric potential difference, which stems from the difference between the two Ag/AgCl electrodes potential and is typically smaller than 1 mV in our experiments. Since it takes more than 100 h for $K^+$ and $Cl^-$ ions to migrate from one reservoir to the other reservoir by electro-osmosis or electrophoresis under 1 mV, we can safely neglect the influence of the small electric potential difference on diffusion experiments. It should be noted that the ionic

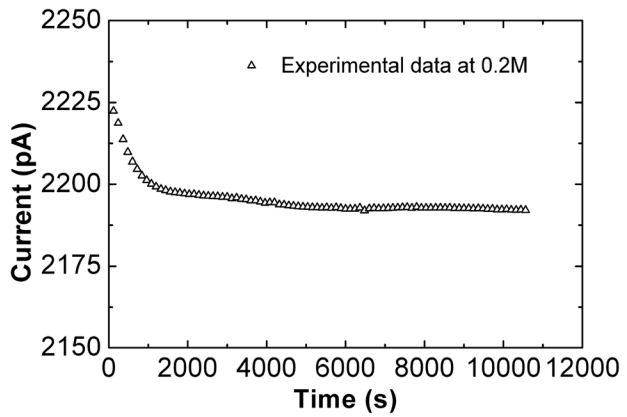


FIG. 4. Ionic current as a function of time for ionic equilibrium at 200 mM.

current also changes rapidly during the first few minutes of diffusion experiments. Indeed, the ionic current only varies within 8 pA from 1200 to 10 560 s. Therefore, our device has enough precision for high concentration experiments.

The initial concentration in the reservoirs was 100 mM. After ionic equilibrium, the solution in the both reservoirs was replaced by a 200 mM solution. The recorded ionic current during diffusion is shown in Fig. 5(a). As discussed in the Theory section, we used the exponential expression $I = I_1 - A\exp(-t/\tau)$ to fit the experimental data after 1200 s and got the characteristic time $\tau = 2396$ s. Then the KCl diffusion coefficient can be estimated as $D = L^2/(\tau \times \pi^2) = 1.52 \times 10^{-9}$ m$^2$/s. Similarly, we got the results for the case in which the solution in the reservoirs was replaced from 200 mM to 100 mM, as shown in Fig. 5(b). The corresponding diffusion coefficient is $D = 1.54 \times 10^{-9}$ m$^2$/s. In Fig. 5, the fitting exponential curves fit the experiment data very well. The current changes fast at the beginning and becomes saturated at the later stage. When the diffusion time reached 12 000 s, which was about five times of the characteristic time $\tau$, we thought that the ion diffusion achieved quasi accomplishment in the nanochannels.

According to the current monitoring method, a series of repeating experiments were conducted and ion diffusion coefficients were obtained as shown in Table I. The KCl diffusion coefficient between 100 mM and 200 mM in the 65-nm-height nanochannels at about 293 K is $D = 1.55 \times 10^{-9}$ m$^2$/s, which is close to its bulk value ($\sim 1.6 \times 10^{-9}$ m$^2$/s).

### B. Medium concentrations

We did the diffusion experiments at medium concentrations similar to the high concentrations. We also used the current monitoring method to obtain the fitting ion diffusion coefficients, which we call the apparent diffusion coefficients. As discussed in the Theory section, unless the change of surface charge and electro-osmotic current can be neglected during

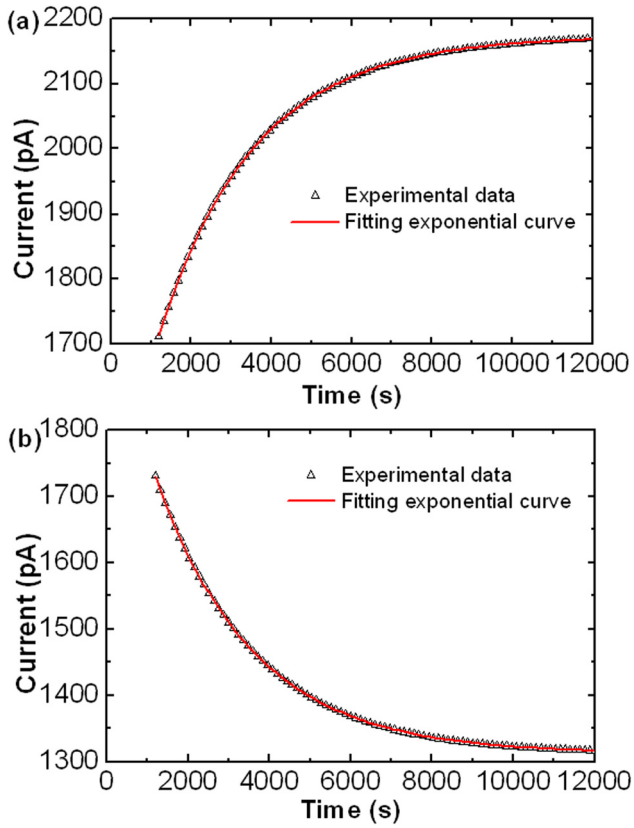


FIG. 5. Ionic current as a function of diffusion time at high concentrations. (a) Diffusion from 100 mM to 200 mM. (b) Diffusion from 200 mM to 100 mM. A mono-exponential expression $I = I_1 - A\exp(-t/\tau)$ is used to fit the experimental data.

TABLE I. Ion diffusion coefficients in the nanochannels between 100 mM and 200 mM.

| No. of experiments | 1 | 2 | 3 | 4 | 5 | 6 |
|---|---|---|---|---|---|---|
| $D$ ($\times 10^{-9}$ m$^2$/s) | 1.52 | 1.54 | 1.66 | 1.51 | 1.53 | 1.51 |

diffusion process, the apparent diffusion coefficients are different from the real diffusion coefficients.

The monitored current during diffusion between 1 mM and 10 mM is shown in Figs. 6(a) and 6(b). By fitting the experimental data, we obtained the apparent diffusion coefficients as about $1.6 \times 10^{-9}$ m$^2$/s, which is also close to its bulk value. However, it should be noted that the corresponding fitting exponential curves did not fit the experimental data so well as those of high concentration experiments. Such deviation is a result of the change of the nanochannel surface charge or the electro-osmotic current.

We further did diffusion experiments at other medium concentrations. The apparent diffusion coefficients and the correlation coefficients are shown in Table II. It is found that the exponential curve tends to fit worse with lower bulk concentration for the whole diffusion process. For a better analysis, we also presented the results of the early period and the later period in Table II. When the bulk concentration was lower than 10 mM, we found that the apparent diffusion coefficients of different periods tend to have significant difference, which made the fitting exponential curves not to fit the experimental data of the whole diffusion process very well.

In order to better understand the experimental phenomena, we used numerical simulation with the PNP equations and the NS equations to analyze the nanochannel conductance at

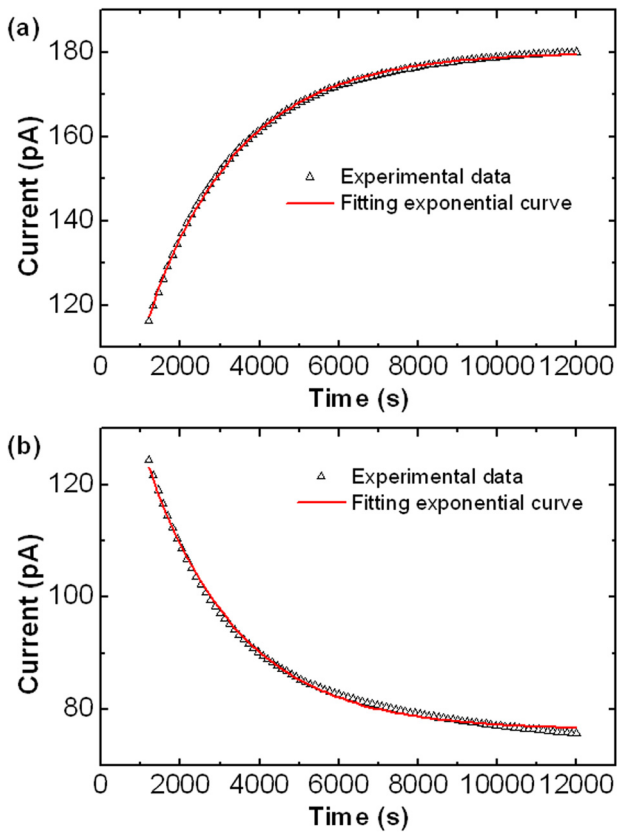


FIG. 6. Ionic current as a function of diffusion time at medium concentrations. (a) Diffusion from 1 mM to 10 mM. (b) Diffusion from 10 mM to 1 mM. A mono-exponential expression $I = I_1 - A\exp(-t/\tau)$ is used to fit the experimental data.

TABLE II. Apparent diffusion coefficients in the nanochannels between 1 mM and 100 mM.

| Experiments | $D$ of the whole process (1200–12 000 s) ($\times 10^{-9}$ m$^2$/s) | $D$ of the early period (1200–4200 s) ($\times 10^{-9}$ m$^2$/s) | $D$ of the later period (9000–12 000 s) ($\times 10^{-9}$ m$^2$/s) |
|---|---|---|---|
| From 10 mM to 100 mM | 1.72(0.99974)[a] | 1.93(0.99996) | 1.63(0.99996) |
| From 100 mM to 10 mM | 1.48(0.99996) | 1.49(0.99997) | 1.54(0.99995) |
| From 1 mM to 10 mM | 1.60(0.99954) | 1.82(0.99998) | 1.18(0.99877) |
| From 10 mM to 1 mM | 1.58(0.99841) | 1.86(0.99999) | 0.53(0.99920) |
| From 2 mM to 5 mM | 1.39(0.99756) | 1.73(0.99997) | 0.20(0.99899) |
| From 1 mM to 2 mM | 0.85(0.99647) | 1.24(0.99978) | 0.83(0.99519) |
| From 2 mM to 1 mM | 1.06(0.99522) | 1.69(0.99950) | 0.40(0.99561) |

[a]The number in brackets, behind the ion diffusion coefficient, is Adjusted R-Square, which is a correlation coefficient of the fitting exponential curve and the experiment data. The better the fitting exponential curve fits the experiment data, the closer to one the value of this correlation coefficient.

different concentrations. The numerical method is similar to that reported in our previous study.[23] At sufficiently low voltages, a nanochannel behaves as a linear ohmic resistor, far from ionic concentration polarization.[55] So we could use a 1-$\mu$m-length nanochannel 2D model to simulate our nanochannels.

The surface charge density of the nanochannel is an important boundary condition for the simulation. Although the charge regulation model gives a better description for surface charge density, the reported values for the parameters in this model have large ranges.[37,38] In addition, the surface charge on the nanochannel walls does not instantaneously achieve equilibrium with solution during our diffusion experiments. Here, the surface charge density of the nanochannel is assumed to be a constant value as $\sigma = -10$ mC/m$^2$, which is comparable to the relevant literatures.[38,39,55]

From Fig. 7(a), it is found that, as the bulk concentration increases, the electrophoretic current increases due to the increase of the total ionic concentration, while the electro-osmotic current deceases due to the decrease of the electro-osmotic velocity. We take A as the ratio of the variation in the electro-osmotic current to the variation in the electrophoretic current during diffusion. From 0.1 mM to 1 mM, A = 54.4%; from 1 mM to 2 mM, A = 8.9%; from 2 mM to 5 mM, A = 4.3%; from 5 mM to 0.01M, A = 1.8%. If the value of A is very small, we can get an approximate linear relationship between the total ionic current and the average ionic concentration.

The average concentrations of each species in the nanochannel at different bulk concentrations are shown in Fig. 7(b). Due to a negative surface charge density of the nanochannel, the $K^+$ concentration is larger than the $Cl^-$ concentration. Because of the electroneutrality requirement, the difference in the average ionic concentrations between $K^+$ and $Cl^-$ is determined by the surface charge density. As the bulk concentration deceases, the surface charge plays a more important role on the total ion concentration. Therefore, the effect of the change of surface charge is more significant at lower bulk concentration.

As can be seen from Table II, the exponential curves did not fit the experimental data of the later periods as well as those of the early periods for bulk concentrations below 10 mM. Since the change of ionic concentration caused by diffusion is small at the later periods, the current caused by the change of surface charge cannot be neglected during the later periods of $c_{bulk} \leq 10$ mM, resulting in bad fittings. Given the fact that the exponential curves fitted experimental data of the early periods very well for $c_{bulk} > 2$ mM, we believe that the effects of the surface charge and the electro-osmotic current are not significant for $c_{bulk} > 2$ mM. As a result, we can take the apparent diffusion coefficients of the early periods as approximate ion diffusion coefficients for $c_{bulk} > 2$ mM. The diffusion coefficients of KCl solution between 2 mM and 100 mM in the nanochannels are about (1.5–1.9) $\times$ $10^{-9}$ m$^2$/s, which are also close to its bulk values.

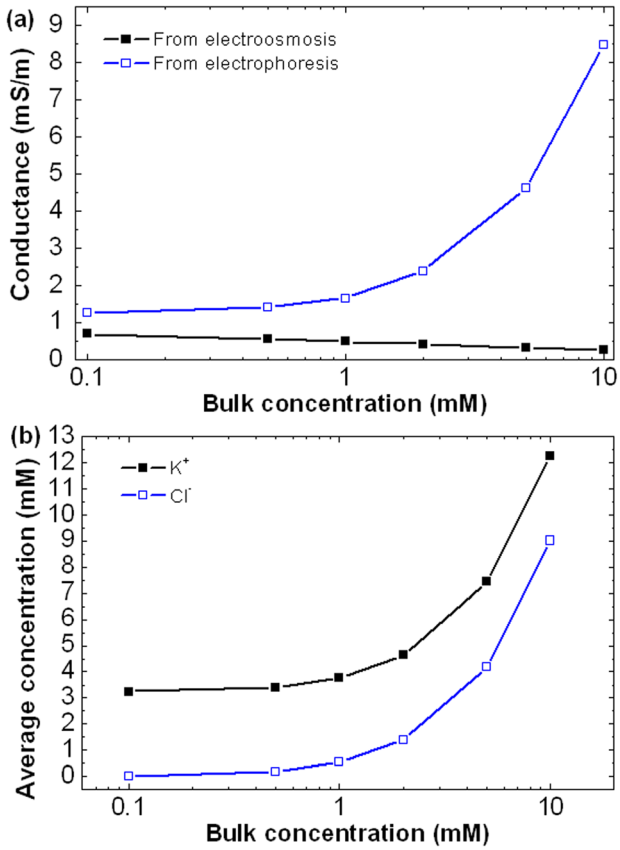


FIG. 7. Numerical results of the 1-$\mu$m-length nanochannel 2D model. (a) The electro-osmotic conductance and the electrophoretic conductance as a function of bulk concentration. (b) Ionic average concentration of each species in the nanochannel as a function of bulk concentration.

### C. Low concentrations

We conducted diffusion experiments at low concentrations below 1 mM, where the thickness of EDL is comparable to the height of the nanochannels and surface conductance dominates the nanochannel conductance. We first checked the reliability of our experimental system with 0.1 mM KCl solution. The ionic current changed less than 0.2 pA in several hours, as shown in Fig. 8(a). Thus, a small variation of ionic current in our low concentration experiments would be valid.

Next, we got the ionic current during the process of diffusion from 0.1 mM to 1 mM, as shown in Fig. 8(b). We find that the exponential curve fitted the experimental data very well at the whole process, which is contrary to the trend at medium concentrations. The corresponding apparent diffusion coefficient is $D = 0.39 \times 10^{-9}$ m$^2$/s, which is significantly smaller than its bulk value. Meanwhile, we note that the current did not reach saturation even after 21 600 s. Comparing with high concentration experiments, it took much more time to achieve apparent diffusion equilibrium at low concentration in our experiments. Although a significant decrease in the real diffusion coefficient of the low concentration solution in nanochannels seems to be a possible reason for the slow apparent diffusion equilibrium, a more possible cause is the slow equilibrium of the nanochannel surface charge since the change of surface charge was already significant at the later periods of $c_{bulk} \leq 10$ mM.

We can simply divide the variation of ionic current during diffusion into two parts: the first one stems from diffusion under constant surface charge, and the second one stems from the change of surface charge. Referring to our experimental results, we assume that: (i) under constant surface charge condition, the variation of ionic current approximately follows a

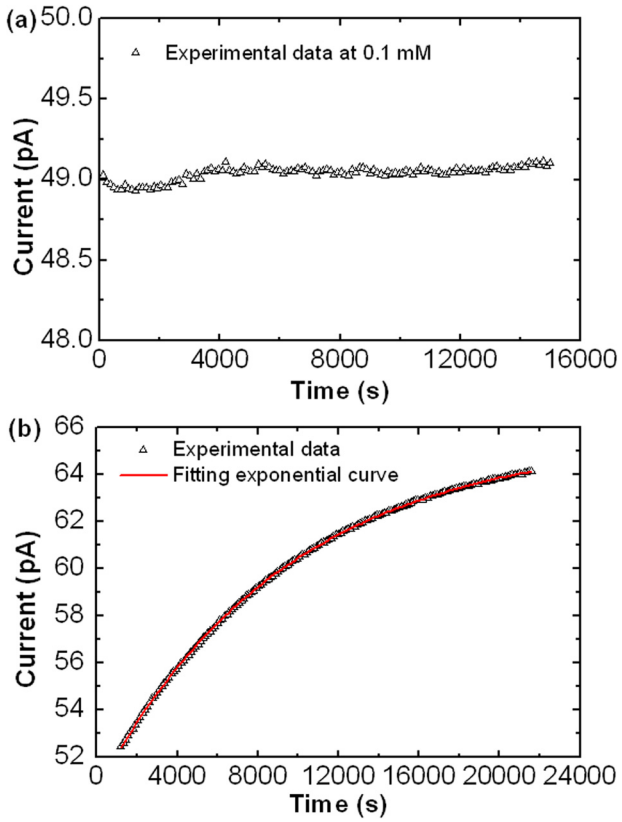


FIG. 8. (a) Ionic current as a function of time for ionic equilibrium at 0.1 mM. (b) Ionic current as a function of diffusion time during diffusion from 0.1 mM to 1 mM.

mono-exponential relation, $\Delta I = -A\exp(-t/\tau)$; (ii) the variation of ionic current stemmed from the change of surface charge also approximately follows a mono-exponential relation, $\Delta I' = -A'\exp(-t/\tau')$.

We hypothesize that the slow equilibrium in the low concentration experiment are caused by the change of the nanochannel surface charge, implying that the characteristic time of the change of surface charge $\tau'$ is larger than that of diffusion $\tau$. Consequently, the effect of surface charge is more significant at the later periods of a diffusion process. As expected, the apparent diffusion coefficients of the later periods during diffusion between 1 mM and 10 mM significantly decreased in our experiments. When the change of surface charge is significant at whole process of low concentration experiment, we can get the good fitting and the small apparent diffusion coefficient in the low concentration experiment.

Further, we used another device with shorter nanochannels to validate our hypothesis above. The device had 30 nanochannels: each is $2.9 \pm 0.1$ mm long, $65 \pm 2$ nm high, and $5 \pm 0.5$ $\mu$m wide (totally $150 \pm 15$ $\mu$m wide). Since the characteristic time of diffusion is $\tau = L^2/(D \times \pi^2)$, the shorter channels have a shorter $\tau$ so that it is easier to separate the ion diffusion dominant period and the surface charge dominant period.

The experimental results of diffusion from 100 mM to 200 mM and diffusion from 0.1 mM to 1 mM are shown in Figs. 9(a) and 9(b). For the high concentration experiment, we got the characteristic time of general diffusion $\tau$ as 532 s. Consequently, we could obtain the KCl diffusion coefficient of high concentrations (100–200 mM) as $1.60 \times 10^{-9}$ m$^2$/s.

For the low concentration experiment, we used a fitting curve $I = -A\exp(-t/\tau) - A'\exp(-t/\tau') + I_1$ to compare with our experimental data, where $-A'\exp(-t/\tau')$ and $I_1$ came from a mono-exponential function fit for the surface charge dominant period (12 000–20 640 s), and $\tau$ was got from the high concentration experiment. As shown in Fig. 9(b), the fitting curve

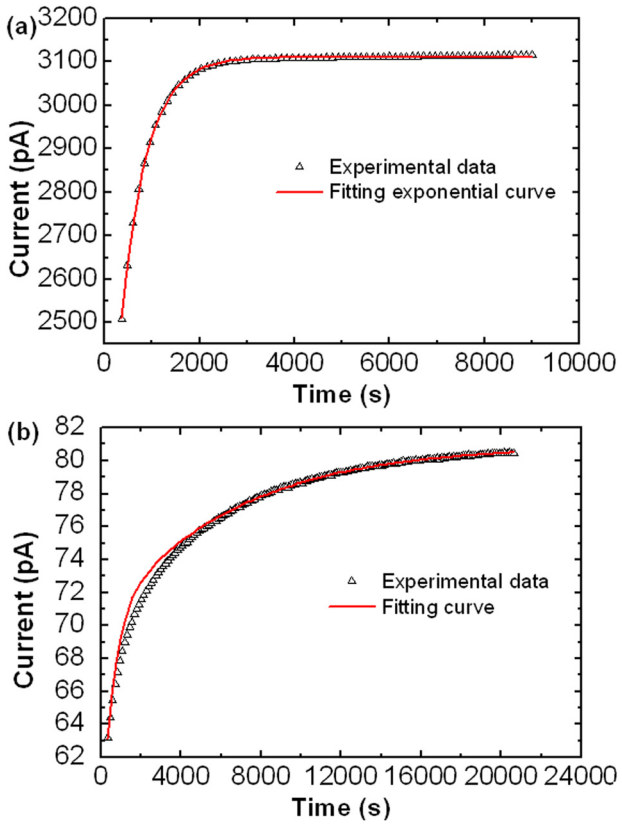


FIG. 9. Ion current as a function of diffusion time for the 2.9-mm-length nanochannels. (a) Diffusion from 100 mM to 200 mM, the fitting exponential curve (red line) is used the mono-exponential expression $I = I_1 - A\exp(-t/\tau)$. (b) Diffusion from 0.1 mM to 1 mM, the fitting curve (red line) is $I = -A\exp(-t/\tau) - A'\exp(-t/\tau') + I_1$, with $A = 14.8$ pA, $\tau = 532$ s, $A' = 10.9$ pA, $\tau' = 6307$ s, $I_1 = 80.9$ pA.

was slightly larger than the experimental data during the ion diffusion dominant period (360–4000 s). We attributed it to the electro-osmotic current, which deceases with increased concentration under constant surface charge.

We had also changed the value of $\tau$ and found that the fitting curve fitted experiment data well with the value of $\tau$ about 900 s and was larger than the experimental data with smaller value during the ion diffusion dominant period. The corresponding apparent diffusion coefficient of fitting parameter $\tau$ for 900 s is $0.95 \times 10^{-9}$ m$^2$/s, which is not significantly smaller than its bulk value. Considering the effect of the electro-osmotic current, we think that the diffusion coefficient of the low concentration KCl solution is also close to its bulk value.

From Fig. 9(b), a good fitting exponential curve is observed at the surface charge dominant period and the characteristic time $\tau'$ is 6307 s. The corresponding apparent diffusion coefficient is $D = 0.14 \times 10^{-9}$ m$^2$/s that is one order of magnitude lower than its bulk value. However, we conclude that it was not the real diffusion coefficient since the change of surface charge dominated the variation of ionic current. Since the variation of ionic current is approximately linear with the change of surface charge density at the surface charge dominant period, the equilibrium rate between the silica nanochannel surface charge and solution approximately follows a mono-exponential relation. Considering the nature of the exponential relation, we estimated that it took about 10 h for the equilibrium between the wall charge and solution.

## V. CONCLUSION

With combined experimental measurement and theoretical analysis, we have investigated the ion diffusion in nanochannels at various solution concentrations. The diffusion process is

observed by monitoring the ionic current through the nanochannel. Our data suggest that the ionic diffusion coefficients in nanochannels at high concentrations are close to their bulk values. By extending the present current monitoring method, the ion diffusion at medium and low concentrations is also obtained. While the ionic diffusion coefficient at medium concentrations is still close to the bulk value, the apparent diffusion coefficients at low concentrations are significantly smaller than their bulk values. We contribute such disparity to the slow change of the nanochannel surface charge. Taking account of the effects of the surface charge equilibrium, the real ionic diffusion coefficient at low concentrations is still at the same order of its bulk value. The equilibrium rate between the silica nanochannel surface charge and solution has been found to follow a mono-exponential relation in our experiments. Our findings suggest that the effects of slow surface charge equilibrium should be considered in the study of ionic transport within nanoscale confinement, especially at low concentrations.

## ACKNOWLEDGMENTS

This work was partially supported by MOST (2011CB707604) and NSFC (11272321, 11102214). We also thank the Nanofabrication Facility at Suzhou Institute of Nano-tech and Nanobionics (SINANO) of Chinese Academy of Science (CAS) for technical support in device fabrication.

[1]J. T. Eijkel and A. Berg, Microfluid. Nanofluid. **1**, 249–267 (2005).
[2]C. H. Duan, W. Wang, and Q. Xie, Biomicrofluidics **7**, 026501 (2013).
[3]R. Schoch, J. Han, and P. Renaud, Rev. Mod. Phys. **80**, 839–883 (2008).
[4]W. Reisner, J. N. Pedersen, and R. H. Austin, Rep. Prog. Phys. **75**, 106601 (2012).
[5]X. Yong and L. T. Zhang, Microfluid. Nanofluid. **14**, 299–308 (2013).
[6]E. Ingelstam, J. Opt. Soc. Am. **47**, 536–543 (1957).
[7]A. Afkhami and F. Khajavi, Sens. Actuator, B Chem. **173**, 620–629 (2012).
[8]G. Gerhardt and R. N. Adams, Anal. Chem. **54**, 2618–2620 (1982).
[9]W. T. Yap and L. M. Doane, Anal. Chem. **54**, 1437–1439 (1982).
[10]J. M. Rosamilia and B. Miller, Anal. Chem. **56**, 2410–2413 (1984).
[11]X. Jiang, N. Mishra, J. N. Turner, and M. G. Spencer, Microfluid. Nanofluid. **5**, 695–701 (2008).
[12]N. F. Y. Durand, C. Dellagiacoma, R. Goetschmann, A. Bertsch, I. Marki, T. Lasser, and P. Renaud, Anal. Chem. **81**, 5407–5412 (2009).
[13]A. Grattoni, D. Fine, E. Zabre, A. Ziemys, J. Gill, Y. Mackeyev, M. A. Cheney, D. C. Danila, S. Hosali, L. J. Wilson, F. Hussain, and M. Ferrari, ACS Nano **5**, 9382–9391 (2011).
[14]W. Im and B. Roux, J. Mol. Biol. **319**, 1177–1197 (2002).
[15]Y. Luo, B. Egwolf, D. E. Walters, and B. Roux, J. Phys. Chem. B **114**, 952–958 (2010).
[16]J. M. Xue, X. Q. Zou, Y. B. Xie, and Y. G. Wang, J. Phys. D: Appl. Phys. **42**, 105308 (2009).
[17]J. N. Israelachvili, *Intermolecular and Surface Forces* (Academic Press, London, 2011).
[18]H. Daiguji, Chem. Soc. Rev. **39**, 901–911 (2010).
[19]S. W. Joo, S. Y. Lee, J. Liu, and S. Z. Qian, ChemPhysChem **11**, 3281–3290 (2010).
[20]S. Y. Lee, S. E. Yalcin, S. W. Joo, O. Baysal, and S. Qian, J. Phys. Chem. B **114**, 6437–6446 (2010).
[21]S. W. Joo and S. Qian, J. Colloid Interface Sci. **356**, 331–340 (2011).
[22]K. L. Liu, J. P. Hsu, and S. Tseng, Langmuir **29**, 9598–9603 (2013).
[23]J. Wang, J. Ma, Z. Ni, L. Zhang, and G. Hu, RSC Adv. **4**, 7601–7610 (2014).
[24]Z. Siwy, I. D. Kosinska, A. Fulinski, and C. R. Martin, Phys. Rev. Lett. **94**, 048102 (2005).
[25]T. Hirono, S. Nakashima, and C. J. Spiers, Int. J. Rock Mech. Min. Sci. **45**, 450–459 (2008).
[26]G. Yossifon and H. C. Chang, Phys. Rev. Lett. **101**, 254501 (2008).
[27]E. A. Bluhm, E. Bauer, R. M. Chamberlin, K. D. Abney, J. S. Young, and G. D. Jarvinen, Langmuir **15**, 8668–8672 (1999).
[28]E. A. Bluhm, N. C. Schroeder, E. Bauer, J. N. Fife, R. M. Chamberlin, K. D. Abney, J. S. Young, and G. D. Jarvinen, Langmuir **16**, 7056–7060 (2000).
[29]B. Xiao, C. Wu, Y. Sun, and Z. Jin, Micro Nano Lett. **4**, 192–197 (2009).
[30]Y. T. Tsai, K. J. Chang, and G. J. Wang, Microsyst. Technol. **19**, 937–944 (2013).
[31]D. Stein, M. Kruithof, and C. Dekker, Phys. Rev. Lett. **93**, 035901 (2004).
[32]R. B. Schoch and P. Renaud, Appl. Phys. Lett. **86**, 253111 (2005).
[33]R. B. Schoch, H. van Lintel, and P. Renaud, Phys. Fluids **17**, 100604 (2005).
[34]D. E. Yates, S. Levine, and T. W. Healy, J. Chem. Soc. Faraday Trans. **70**, 1807–1818 (1974).
[35]S. H. Behrens and D. G. Grier, J. Chem. Phys. **115**, 6716–6721 (2001).
[36]F. Baldessari and J. G. Santiago, J. Colloid Interface Sci. **325**, 526–538 (2008).
[37]F. van der Heyden, D. Stein, and C. Dekker, Phys. Rev. Lett. **95**, 116104 (2005).
[38]F. H. J. van der Heyden, D. J. Bonthuis, D. Stein, C. Meyer, and C. Dekker, Nano Lett. **7**, 1022–1025 (2007).
[39]Y. S. Choi and S. J. Kim, J. Colloid Interface Sci. **333**, 672–678 (2009).
[40]M. Wang and A. Revil, J. Colloid Interface Sci. **343**, 381–386 (2010).
[41]T. A. Zangle, A. Mani, and J. G. Santiago, Langmuir **25**, 3909–3916 (2009).

[42]S. I. Raider, L. V. Gregor, and R. Flitsch, J. Electrochem. Soc. **120**, 425–431 (1973).
[43]C. H. Duan and A. Majumdar, Nat. Nanotechnol. **5**, 848–852 (2010).
[44]H. S. Harned and R. L. Nuttall, J. Am. Chem. Soc. **71**, 1460–1463 (1949).
[45]A. Sze, D. Erickson, L. Ren, and D. Li, J. Colloid Interface Sci. **261**, 402–410 (2003).
[46]S. W. Tang, C. H. Chang, and H. H. Wei, Microfluid. Nanofluid. **10**, 337–353 (2011).
[47]H. S. Harned and R. L. Nuttall, J. Am. Chem. Soc. **69**, 736–740 (1947).
[48]Y. Wang, K. Pant, Z. Chen, G. Wang, W. F. Diffey, P. Ashley, and S. Sundaram, Microfluid. Nanofluid. **7**, 683–696 (2009).
[49]J. Koryta, J. Dvorak, and L. Kavan, *Principles of Electrochemistry* (Wiley, New York, 1993).
[50]D.-K. Kim, C. Duan, Y.-F. Chen, and A. Majumdar, Microfluid. Nanofluid. **9**, 1215–1224 (2010).
[51]X. Xuan and D. Li, Electrophoresis **27**, 5020–5031 (2006).
[52]A. S. Khair and T. M. Squires, J. Fluid Mech. **615**, 323–334 (2008).
[53]J. Fu, P. Mao, and J. Han, Nat. Protoc. **4**, 1681–1698 (2009).
[54]P. Mao and J. Han, Lab Chip **5**, 837–844 (2005).
[55]H. C. Chang and G. Yossifon, Biomicrofluidics **3**, 12001 (2009).